ImmunoHorizons

RESEARCH ARTICLE

Infectious Disease

# FIBCD1 Deficiency Decreases Disease Severity in a Murine Model of Invasive Pulmonary Aspergillosis

**Shreya Bhattacharya,[*,†] Nansalmaa Amarsaikhan,[*,‡] Alec J. Maupin,[*] Anders Schlosser,[§,¶] Ernst-Martin Füchtbauer,[‖] Uffe Holmskov,[§,¶] Jesper Bonnet Moeller,[§,¶,#] and Steven P. Templeton[*]**

[*]Department of Microbiology and Immunology, Indiana University School of Medicine–Terre Haute, Terre Haute, IN; [†]Department of Biology, Indiana State University, Terre Haute, IN; [‡]Department of Pediatrics, Indiana University School of Medicine, Indianapolis, IN; [§]Department of Cancer and Inflammation Research, University of Southern Denmark, Odense, Denmark; [¶]Department of Molecular Medicine, University of Southern Denmark, Odense, Denmark; [‖]Department of Molecular Biology and Genetics, Aarhus University, Aarhus, Denmark; and [#]Danish Institute for Advanced Study, University of Southern Denmark, Odense, Denmark



## ABSTRACT

*Aspergillus fumigatus* is a ubiquitous mold associated with the development of pulmonary diseases that include invasive pulmonary aspergillosis (IPA), an often fatal opportunistic infection. FIBCD1 is a transmembrane endocytic membrane receptor widely expressed on human epithelium. Although FIBCD1 was previously shown to bind chitin, modulate fungal colonization of the gut, and inhibit intestinal inflammation, the role of FIBCD1 in the context of lung fungal infection remains unknown. In this study, we observed that mortality, fungal burden, and tissue histopathology were decreased in the absence of FIBCD1 in murine IPA. Quantitative RT-PCR analyses demonstrated decreased inflammatory cytokines in the lungs of neutrophil-depleted FIBCD1$^{-/-}$ mice with IPA, when compared with wild-type controls. In contrast, inflammatory cytokines were increased in immune-competent FIBCD1$^{-/-}$ mice after fungal aspiration, suggesting that the presence of neutrophils is associated with cytokine modulation. In contrast to the clear IPA phenotype, FIBCD1$^{-/-}$ mice with systemic infection or bleomycin-induced lung injury exhibited similar morbidity and mortality when compared with their wild-type counterparts. Thus, our study identifies a detrimental role of FIBCD1 in IPA. *ImmunoHorizons*, 2021, 5: 983–993.

## INTRODUCTION

*Aspergillus fumigatus* is a filamentous fungus associated with inflammatory pulmonary diseases and opportunistic infection in immunocompromised individuals (1). It is abundant in indoor and outdoor environments, and asexual airborne conidia are frequently inhaled (2). Upon inhalation and subsequent germination, immune-stimulatory cell wall components masked by an inert hydrophobic rodlet layer are exposed (3). The early immune responses in lungs to inhaled *Aspergillus* conidia consist of innate recognition of these fungal cell wall components via fungal pattern recognition receptors (PRRs). Interactions between fungal pathogen-associated molecular patterns and their cognate PRRs initiate early inflammatory responses in the host (4–7). Immune-competent hosts successfully eliminate inhaled fungi by smooth muscle contraction and phagocytosis by resident alveolar macrophages and infiltrating neutrophils. However, in case of immunocompromised or immune-deficient individuals, *A. fumigatus* hyphae penetrate the lung parenchyma, resulting in invasive pulmonary aspergillosis (IPA) (8–10). In patients with IPA, *A. fumigatus* can disseminate and invade heart, liver, and brain tissues and is often fatal.

Received for publication October 18, 2021. Accepted for publication December 3, 2021.

**Address correspondence and reprint requests to:** Dr. Steven P. Templeton, Indiana University School of Medicine–Terre Haute, 620 Chestnut Street, HH135, Terre Haute, IN 47809. E-mail address: sptemple@iupui.edu

ORCIDs: 0000-0001-8786-8037 (J.B.M.); 0000-0003-3430-7011 (S.P.T.).

**Abbreviations used in this article:** B6, C57BL/6; BALF, bronchoalveolar lavage fluid; DSS, dextran sodium sulfate; GMS, Gomori's modified methenamine silver; IA, invasive aspergillosis; IPA, invasive pulmonary aspergillosis; LDH, lactate dehydrogenase; PRR, pattern recognition receptor; qPCR, quantitative PCR; qRT-PCR, quantitative RT-PCR.

The online version of this article contains supplemental material.



https://doi.org/10.4049/immunohorizons.2100092

Fungal PRRs include the well-studied C-type lectin receptor dectin-1, which recognizes the cell-wall carbohydrate β-glucan. Dectin-1 has been shown to play an important role in anti-fungal immunity through activation of the Syk/CARD9 pathway (3, 4, 11). In contrast to β-glucan, less is known about pattern recognition of chitin, the second most abundant biopolymer on earth. FIBCD1 is a chitin-binding membrane-bound protein that is expressed on the human lung epithelium and on the apical surface of intestine (12). Recombinant FIBCD1 has been shown to bind exposed cell-wall chitin of opportunistic fungal pathogens such as *A. fumigatus* and *Candida* spp. in vitro, and epithelial-specific FIBCD1 expression in mice has been shown to regulate intestinal fungal colonization and ameliorate dextran sodium sulfate (DSS)–mediated gut inflammation (13–17). However, the role of FIBCD1 in pulmonary fungal infection still remains elusive. In this study, we generated FIBCD1-deficient (Fibcd1$^{-/-}$) mice to investigate the role of this molecule in *A. fumigatus* inhalation, infection, inflammatory pathology, and lung injury.

## MATERIALS AND METHODS

### *Growth and handling of fungi*

The clinical isolate of *A. fumigatus* Af293 was purchased from the Fungal Genetics Stock Center, and CEA10 was provided by Dr. Robert Cramer (Geisel School of Medicine at Dartmouth). Isolate Af293 was cultured on malt extract agar, and CEA10 was cultured on glucose minimal medium plates. Conidia were isolated from culture plates kept at 24 or 37°C for 14 d by applying and gently shaking 1 g of glass beads (0.5 mm, BioSpec Products), then placed in suspension by pouring the beads into a tube with sterile PBS. The beads were then vortexed and the supernatant containing the conidia was removed, diluted, and counted with a hemacytometer for further experimental procedures (18, 19).

### *Generation of Fibcd1$^{-/-}$ mice*

Fibcd1$^{-/-}$ mice were produced by targeting exon 2 of Fibcd1. In brief, flanking regions of exon 2 were amplified by PCR using the primer pairs 5′-TAGAATTCCACAGGCCATGTGGATACCACACA-3′/5′-TAGAATTCCACAGGACATAACTGCAGCTTGCTC-3′ and 5′-TACCCGGGCCGACACCCTGTGCTGAATTATAA-3′/5′- TACCCGGGATCCCCACATGAAGGAGGCTAAGG-3′, and subsequently cloned into the vector pKO Scrambler NTKV-1903 (Agilent Technologies) using the restriction nucleases EcoRI and SmaI, respectively. Following verification by sequencing, the prepared targeting vector was linearized and electroporated into CJ7 embryonic stem cells (20) using a Gene Pulser (Bio-Rad). Electroporation conditions were as follows: 240 V and 500 mF. Cells were selected using 350 mg/ml G418 and 0.5 μM FIAU, and homologous recombinants were identified by Southern blotting and PCR. Chimeric mice were generated by injection of targeted embryonic stem cell clones into B6D2F2 blastocysts to obtain mice heterozygously transmitting the Fibcd1-knockout variant. Their descendants were backcrossed to C57BL/6 (B6) mice (Charles River Laboratories) for 10 generations and maintained as heterozygotes. The heterozygous mice were intercrossed to produce homozygous wild-type and Fibcd1$^{-/-}$ offspring. Fibcd1$^{-/-}$ mice were bred at the Indiana University School of Medicine–Terre Haute animal facility with offspring used in subsequent experiments at 7–10 wk of age. Wild-type B6 mice were obtained from The Jackson Laboratory and were allowed to rest 2–4 wk prior to experiments.

### *Fungal aspiration, infection, and lung harvest*

To induce IPA in mice, neutrophils were depleted by i.p. injection of 0.25 mg of anti-Ly6G (1A8; Bio X Cell) 24 h before and postinfection (21), or mice were treated with cyclophosphamide monohydrate (EMD Millipore; 150 mg/kg of body weight of mouse) 4 and 1 d prior to infection. Immunocompromised mice were infected with 1 × $10^7$ conidia of *A. fumigatus* isolates by involuntary aspiration, as previously described (22, 23). In some experiments, infected mice were monitored for survival for 12 d postinfection. Infected mice were euthanized between 0 and 72 h postinfection with sodium pentobarbital, and lungs were perfused with 10 ml of phosphate PBS. Lungs were harvested for quantification of fungal burden, flow cytometric analysis, lactate dehydrogenase (LDH) quantification, cytokine ELISA, and quantitative RT-PCR (qRT-PCR) assays or histological staining and analysis. Bronchoalveolar lavage was performed to collect samples to assay immune cell composition by flow cytometry. Conidial suspensions were delivered by involuntary aspiration of 5 × $10^7$ conidia for single aspiration. Mice were euthanized at 24 h postchallenge as described previously (22). To induce lung injury, mice were challenged with bleomycin by involuntary aspiration (1.72 mg/ml) and monitored for mortality. Mice from both groups were harvested at days 6 and 13 posttreatment. Bronchoalveolar lavage fluid (BALF) and lungs were collected for further analysis of recruitment of immune cells and cytokine production, as described previously (22). For systemic infection, wild-type and Fibcd1$^{-/-}$ mice were infected retro-orbitally (i.v.) with 5 × $10^6$ *Aspergillus* conidia suspension. Some mice were monitored for survival, whereas others were harvested at day 2 postinfection, and brain, heart, lungs, kidney, and spleen were collected for fungal burden analysis. All animal handling and experimental procedures were performed in accordance with the recommendations found in the *Guide for the Care and Use of Laboratory Animals* of the National Institutes of Health. The work in this study was approved by the Institutional Animal Care and Use Committee of the host campus of Indiana University School of Medicine–Terre Haute, Indiana State University, protocol 1507790-2.

### *Histology*

For paraffin-embedded histological preparation, infected lungs were perfused with 5 ml of saline and then 5 ml of 10% formalin-buffered saline followed by inflation using a tracheal catheter insertion and injection of 1 ml of formalin-buffered saline. The lungs were removed and fixed overnight in formalin-

buffered saline, followed by tissue embedding, processing, and sectioning (Terre Haute Regional Hospital pathology laboratory). To visualize lung infiltration by inflammatory cells, H&E stains were prepared and Gomori's modified methenamine silver (GMS) stain was used for visualization of fungal germination in the lungs, following deparaffinization. The slides were mounted on Cytoseal XYL (8312-4, Thermo Scientific) and viewed under an Olympus SC50 (brightfield camera) using cellSens 64-bit version 3.1 for histological imaging and quantification.

### *Flow cytometric analysis of BALF and lung homogenates*

BALF and lung cell composition were determined by flow cytometric analysis of recovered lavage cells in suspension and stained with surface markers. In brief, lung homogenates were treated with collagenase type IV (Worthington Biochemical) and were incubated in a C25 incubator shaker (New Brunswick Scientific) at 37°C for 35 min and strained through a sterile cell strainer (Thermo Fisher Scientific, 70-μm nylon mesh). The resulting flowthrough was centrifuged for 2 min at 2000 rpm, the supernatant was saved for assays, and the cell pellet was resuspended and washed in 1 ml of FACS buffer (PBS, 5% FBS, 0.05% sodium azide). BALF was centrifuged for 2 min at 2000 rpm, the supernatant was removed, and the cell pellet was resuspended and washed in 1 ml of FACS buffer (PBS, 5% FBS, 0.05% sodium azide). The washed pellet was resuspended and stained in a solution containing FACS buffer with 10% rat serum, Fc receptor blocking Ab (clone 24G2), and the following Abs (BD Biosciences): rat anti-mouse Ly6G-PE-Cy7, rat anti-mouse Siglec-F-PE, pan-leukocyte rat anti-mouse CD45-PerCP, and rat anti-mouse CD11c-allophycocyanin. For T cell population staining, the following Abs were used: rat anti-mouse CD4-allophycocyanin and CD8-FITC (BD Biosciences). Neutrophils were defined as $CD45^{hi}Ly6G^{+}$, eosinophils were defined as $CD45^{hi}Ly6G^{-}CD11c^{-}Siglec\text{-}F^{+}$, and alveolar macrophages were defined as $CD45^{hi}Ly6G^{-}CD11c^{+}Siglec\text{-}F^{+}$. Flow cytometry was performed on a Guava easyCyte 8HT (EMD Millipore).

### *Intracellular cytokine staining*

T cell cytokine production on a per-cell level was determined by fluorescent intracellular cytokine staining as previously described (19). Briefly, the BALF suspension was centrifuged for 2 min at 2000 rpm and washed in 1 ml of complete RP10 medium. The supernatant was discarded and a solution of leukocyte activation cocktail with GolgiPlug (BD Biosciences) was added to each sample for stimulation of cytokine production and simultaneous inhibition of cytokine secretion. Cells were incubated at 37°C for 4 h. After the incubation, cells were washed in FACS buffer and stained for flow cytometric analysis using the surface Abs rat anti-moue CD4-PerCP and rat-anti-mouse CD8-FITC on ice (eBioscience). After a 30-min incubation, cells were washed in FACS buffer and centrifuged, and cell pellets were resuspended in BD Cytofix/Cytoperm for 15 min to allow fixation and permeabilization for subsequent intracellular cytokine staining. Cells were washed and resuspended in BD Perm/Wash (BD Biosciences). Each sample was divided into two tubes and stained with rat anti-mouse IFN-γ-allophycocyanin (eBioscience) and rat anti-mouse IL-17A-PE, or with control isotype Abs (eBioscience). $CD4^{+}$ T cells were defined on the basis of forward and side light scatter and surface CD4 expression. The number of cytokine-producing $CD4^{+}$ T cells was determined by fluorescent intracellular cytokine staining with Abs specific for IFN-γ and IL-17A.

### *Fungal burden assay*

To quantify fungal burden, harvested lungs or organs were rapidly frozen in liquid nitrogen. Genomic DNA was extracted from 50 to 100 mg of freeze-dried, homogenized lung tissue using a previously described DNA extraction buffer for *Aspergillus* nucleic acids with subsequent phenol/chloroform extraction (21, 22). A total of 500 ng of genomic DNA was used for quantitative PCR (qPCR) to determine the fungal DNA content. A qPCR fungal burden assay was performed to determine the amount of fungal 18S rRNA-encoding DNA in lung extracts with 18S rRNA-encoding DNA primer and probe sets with a modified probe quencher (5′-/56-FAM/AGC CAG CGG/ZEN/CCC GCA AAT G/3IABkFQ/-3′). A standard curve was prepared from Af293 genomic DNA and used to calculate the concentration of fungal DNA in each sample, with uninfected mouse lungs analyzed to confirm the absence of contamination. Samples were amplified in triplicate with at least four biological replicates from different mice. The qPCR reaction was performed in an Agilent Mx3005P with MxPro software (Agilent Technologies), and CFX Connect real-time PCR cycle threshold values were used to calculate the corresponding fungal DNA content in the lung tissue, and the fungal burden was reported as nanograms of fungal DNA per milligram of total lung DNA.

### *Total RNA processing and gene expression analysis*

Lungs or organs were removed and flash frozen in liquid nitrogen for RNA extraction. Total RNA was extracted from lungs homogenized in TRIzol reagent (Invitrogen). Following the aqueous upper phase separation, further RNA purification was performed using a Qiagen RNeasy column with on-column DNase treatment per the manufacturer's recommendations. Five micrograms of total RNA was transcribed using a high-capacity cDNA synthesis kit (Life Technologies) according to the manufacturer's protocol. For qPCR, PowerUp SYBR Green PCR master mix (Applied Biosystems) was used with an Mxp3500 real-time PCR system (Agilent Technologies) or CFX Connect real-time PCR. Mouse β-actin was used as a housekeeping gene for cytokine analysis in the murine model. Most primers were designed through Primer3 software from the whole sequence available at GenBank.

### *ELISA and LDH*

Lung homogenates were prepared as mentioned earlier. Supernatants were collected after spinning down the flowthrough.

Supernatants from BALF were also collected after spinning down the BALF. An ELISA was performed on supernatants for some cytokines (PeproTech) as directed by the manufacturer. An LDH cytotoxicity assay was performed on the supernatants to assess tissue damage due to infection, as per the manufacturer's instructions (Thermo Scientific Pierce cytokine kit). To measure lung leakage, albumin concentration was measured using a bacillus Calmette-Guérin albumin assay kit (MilliporeSigma) as per the manufacturer's protocol. Wavelengths emitted from all the assays mentioned above were measured with a plate reader (BioTek Epoch Take3 micro-volume plate reader).

### *Genotyping of Fibcd1 deficiency by Southern blotting and PCR*

Genomic DNA was isolated and ~5 mg was digested with 50 U of either KpnI or HindIII/NdeI, respectively (20). Digested products were separated by electrophoresis using a 0.7% (w/v) agarose gel. Southern blotting was performed by capillary transfer overnight onto a Hybond-N+ membrane (GE Healthcare). Prehybridization, hybridization, and washing procedures were performed at 65°C. After washing, the membranes were placed on Saran Wrap and exposed to double-coated Hyperfilm MS (GE Healthcare) with an intensifying screen for 48 h at −80°C. The probes used for Southern blotting (probes A and B) were generated by conventional PCR using the primer pairs 5′-GTGTGGGGGCTGGAGTTTGGTG-3′/5′-GGGGGCCGGTCCTG-TTCTTGA-3′ and 5′-GCCCTTCCAGCAGCCAGCATAGTAA-3′/5′-CTTCCCCACCCCATCCCTGTTTGA-3′, respectively. Radioactive labeling of the probes were performed using (α-[$^{32}$P])dCTP (GE Healthcare) and the Prime-It II random primer labeling kit as described by the manufacturer (Stratagene).

For multiplex PCR genotyping, DNA was extracted from tail biopsies using the RedExtract-N-Amp kit (Sigma-Aldrich) according to the manufacturer's recommendations. Multiplex PCR was performed using the primers a, 5′-GAGTGAGCAC-CAGGCACAGC-3′, b, 5′-GGATGTGAGAACACACCCTCCA-3′, and c, 5′-GCTCCAGACTGCCTTGGGAA-3′ for the amplification of the wild-type and mutant alleles. Primers a and b amplify a 417-bp fragment corresponding to the wild-type allele, whereas primers a and c amplify a 203-bp fragment corresponding to the mutant allele. Amplification was performed according to the following: 3 min at 95°C; 35 cycles of 95°C (20 s), 65.5°C (30 s), and 72°C (30 s); and a final 3-min elongation at 72°C. The PCR product was separated on 1% agarose gel.

### *Data analysis methods*

GraphPad Prism was used for generation of graphs and figures and for statistical analyses (GraphPad Software). Unpaired *t* tests were used to measure statistical significance when two groups were compared, and one- or two-way ANOVA tests were used along with Tukey posttests for multiple comparisons, respectively. Differences between experimental groups that resulted in a *p* value $<0.05$ were considered significant. Survival curves were analyzed with Mantel–Cox log-rank tests. Analysis of mouse flow cytometric data were performed with FlowJo software, version 10 (Becton-Dickinson). For quantification of fungal growth using histological sections, the mean of four representative fields at ×100 magnification of GMS$^{+}$ staining for each sample was calculated using Olympus cellSens 64-bit version 3.1.

## RESULTS

### *Absence of FIBCD1 increases survival and decreases fungal burden in a murine model of invasive aspergillosis*

FIBCD1 is found in human lung epithelium and modulates lung epithelial inflammatory responses to *A. fumigatus* cell wall polysaccharides, inflammatory mediators, and mucins (13–17). However, the role of FIBCD1 in lung fungal infection remains unknown. In order to determine the role of FIBCD1 in IPA, we generated Fibcd1$^{-/-}$ mice by gene-targeted deletion (Supplemental Fig. 1). To produce the immune-compromised phenotype and invasive infection, we infected neutrophil-depleted or cyclophosphamide-treated wild-type and Fibcd1$^{-/-}$

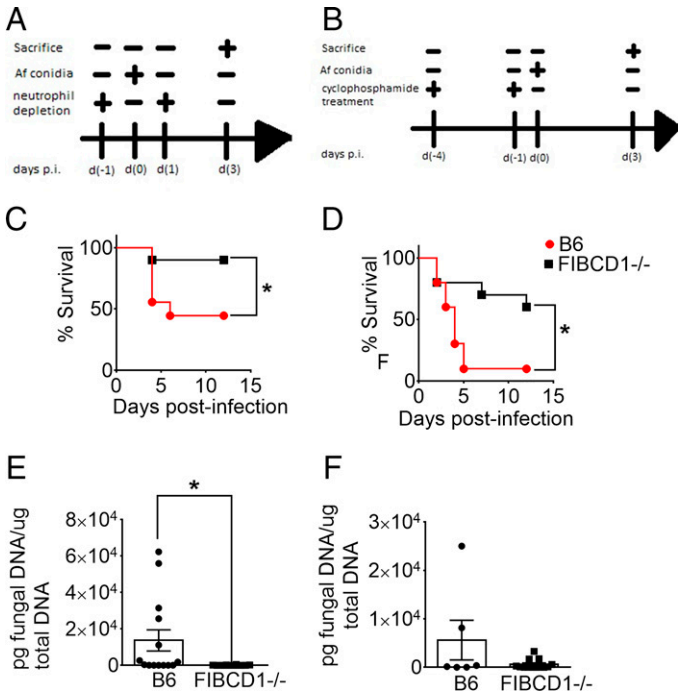


**FIGURE 1. Fibcd1 deficiency increases survival and decreases fungal burden in murine IPA.**

(**A** and **B**) Experimental time courses for different models of infection: neutropenic model (A), cyclophosphamide-treated model (B). (**C** and **D**) Survival score was determined as described in *Materials and Methods*: neutropenic (C), cyclophosphamide treated (D). (**E** and **F**) Quantification of fungal DNA from lung fungal homogenates: neutropenic (E), cyclophosphamide treated (F). $n = 9$–10 mice per group. Data are a summary of three to four independently performed experiments. *$p < 0.05$.

mice with *A. fumigatus* by involuntary aspiration (Fig. 1A, 1B). We observed increased survival in Fibcd1$^{-/-}$ mice, both in neutrophil-depleted and cyclophosphamide-treated mice (Fig. 1C, 1D). When fungal DNA in the lungs of wild-type and Fibcd1$^{-/-}$ mice was quantified by qPCR at day 3 postinfection, a significant decrease was observed in neutropenic Fibcd1$^{-/-}$ mice (Fig. 1E), but did not reach significance with cyclophosphamide treatment (Fig. 1F). Thus, with two different methods of immune suppression, FIBCD1 deficiency results in ameliorated disease in IPA.

### *Lung cytokine modulation due to FIBCD1 in immunocompromised mice with invasive aspergillosis*

Using quantitative RT-PCR, we quantified lung expression of cytokines and immune modulatory genes in wild-type and Fibcd1$^{-/-}$ mice at 72 h postinfection. We observed a decrease in inflammatory cytokine mRNA and protein expression in Fibcd1$^{-/-}$ mice (Fig. 2), consistent with decreased morbidity, mortality, and fungal burden. More specifically, transcription of IL-1β, TNF, IL-6, and IL-23 were decreased in Fibcd1$^{-/-}$ mice by day 3 postinfection (Fig. 2A), and the decrease in Fibcd1$^{-/-}$

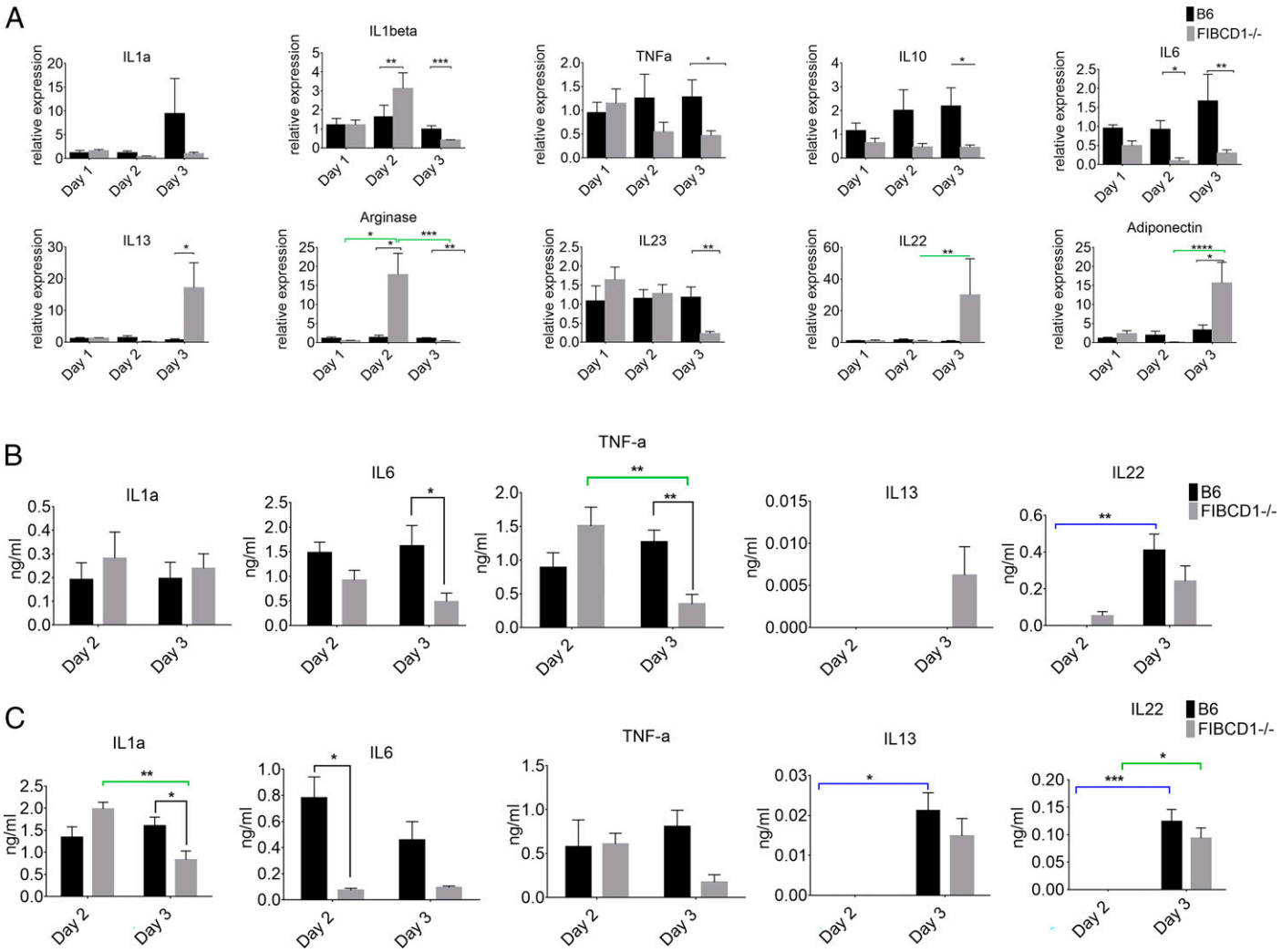


**FIGURE 2. Lung cytokine modulation in immunocompromised Fibcd1$^{-/-}$ mice with IPA.**

Mice of both groups were made immunocompromised and infected with 1 × 10$^7$ Af293 conidia, as described in *Materials and Methods*. BALF and lungs were harvested at days 1, 2, and 3 postinfection to determine modulation of cytokine production. (**A**) qRT-PCR of extracted mRNA from harvested lungs of neutropenic mice at the indicated days postinfection. (**B** and **C**) Cytokine secretion in BALF (B) and lungs (C) of neutropenic mice quantified at the protein level by ELISA. Data are a summary of three to four independently performed experiments and analyzed by an unpaired *t* test or two-way ANOVA multiple test comparison (blue or green bar represents significant difference between days in wild-type or Fibcd1$^{-/-}$ mice, respectively). *$p < 0.05$, **$p < 0.01$, ***$p < 0.001$.

mice was confirmed at the protein level for IL-6 and TNF in BALF (Fig. 2B) and for IL-6 in the lung homogenates. Transcription of adiponectin, an anti-inflammatory adipokine, was increased in the absence of FIBCD1 at day 3 postinfection, yet the other anti-inflammatory cytokine we measured, IL-10, was decreased. Of all of the other cytokines measured in the lungs of Fibcd1$^{-/-}$ mice, only transcription of IL-13 and IL-22 was increased in Fibcd1$^{-/-}$ mice (Fig. 2A). However, we were unable to confirm this increase at the protein level in BALF or lung homogenates (Fig. 2B and 2C, respectively). Our results demonstrate decreased inflammatory cytokine production in Fibcd1$^{-/-}$ mice with IPA.

### *Decreased lung pathology and fungal growth in absence of FIBCD1 in murine model with invasive aspergillosis*

To compare histopathology and lung hyphal invasion in wild-type and Fibcd1$^{-/-}$ mice, lung tissue from infected neutropenic Fibcd1$^{-/-}$ and B6 mice was harvested at day 1 and day 3 postinfection. At day 1 postinfection, numerous swollen and dormant conidia were visible in the lungs of both wild-type and Fibcd1$^{-/-}$ mice in GMS-stained tissue sections (Fig. 3A, top panels), inducing significant infiltration of inflammatory cells in H&E-stained sections (Fig. 3C, top panels). However, by day 3 postinfection, decreased lung fungal growth and tissue inflammation were observed in the lungs of Fibcd1$^{-/-}$ mice when compared with wild-type mice (Fig. 3A, 3C, bottom panels). H&E sections in wild-type mice displayed bronchoalveolar foci with infiltration of leukocytes compared with decreased infiltration in FIBCD1$^{-/-}$ mice (Fig. 3C, bottom panels). In GMS-stained sections, invasive hyphal growth was observed in or near bronchoalveolar spaces, particularly in wild-type mice, and less evident invasive growth in Fibcd1$^{-/-}$ mice (Fig. 3A, bottom panels). When GMS staining was quantified using by an image analysis program, lung fungal staining was equivalent between groups at day 1 postinfection and significantly decreased in Fibcd1$^{-/-}$ mice compared with wild-type mice at day 3 postinfection (Fig. 3B). Lung leakage, measured by albumin in lung BALF, was decreased in Fibcd1$^{-/-}$ mice with invasive aspergillosis (IA) when compared with wild-type mice, although differences in lung damage measured with LDH were not significant (Supplemental Fig. 2). These results suggest increased fungal clearance and decreased fungal pathology in Fibcd1$^{-/-}$ mice with IPA.

### *No significant role of FIBCD1 in immune cell recruitment in IPA*

To explore the effect of FIBCD1 on airway immune cell recruitment in IPA, BALF cells were harvested at day 3 postinfection, placed in suspension, and stained and analyzed by flow cytometry. In BALF cells, no significant differences in eosinophils and alveolar macrophages were observed in wild-type and FIBCD1$^{-/-}$ mice in either neutropenic (Fig. 4A–E) or cyclophosphamide (Fig. 4F–J) models. Thus, despite decreased mortality, fungal burden, and tissue histopathology, airway inflammatory cells were not significantly decreased in the absence of FIBCD1 in mice with IPA.

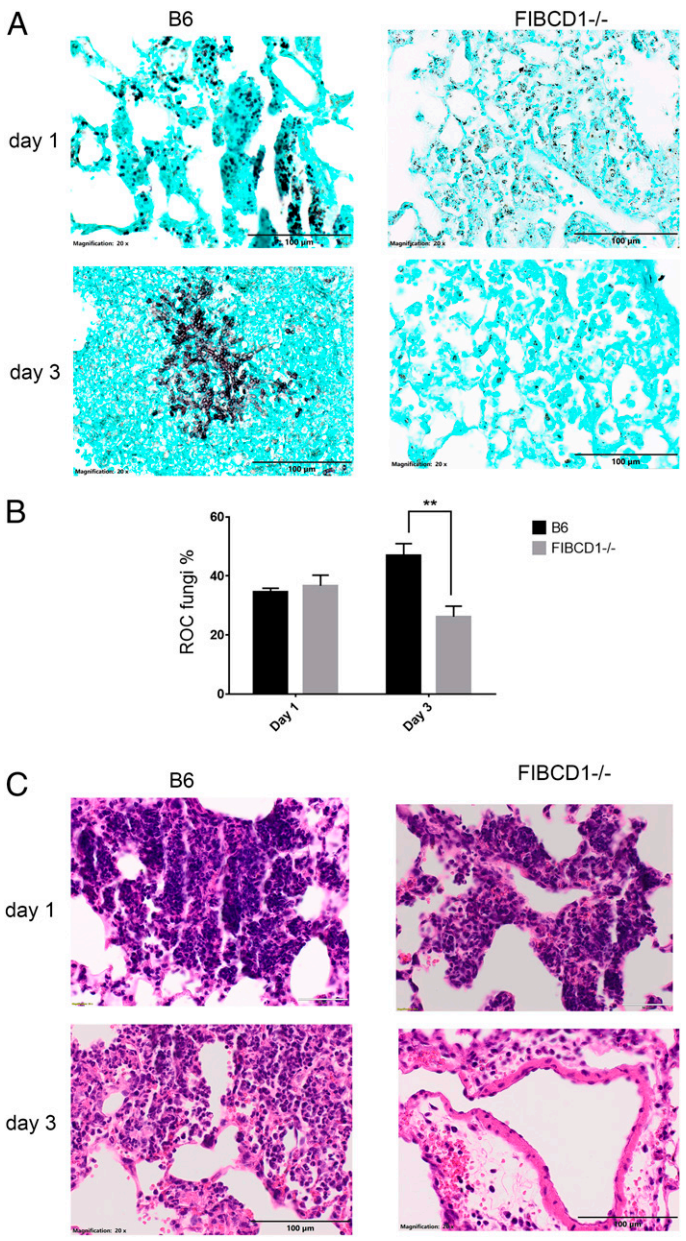


**FIGURE 3. Decreased lung pathology and fungal growth in neutropenic Fibcd1$^{-/-}$ mice with IPA.**

(**A** and **C**) Representative fungal morphology in GMS-stained (A) and H&E-stained (C) sections from control and Fibcd1$^{-/-}$ mice (left and right panels) at days 1 and 3. (**B**) Comparison of fungal burden [receiver operating characteristic (ROC)] as measured by quantification of GMS staining of histological sections ($n$ = 5–6 mice/group) at days 1 and 3. Scale bars, 100 μm. Data are a summary of two to three independently performed experiments. **$p < 0.01$.

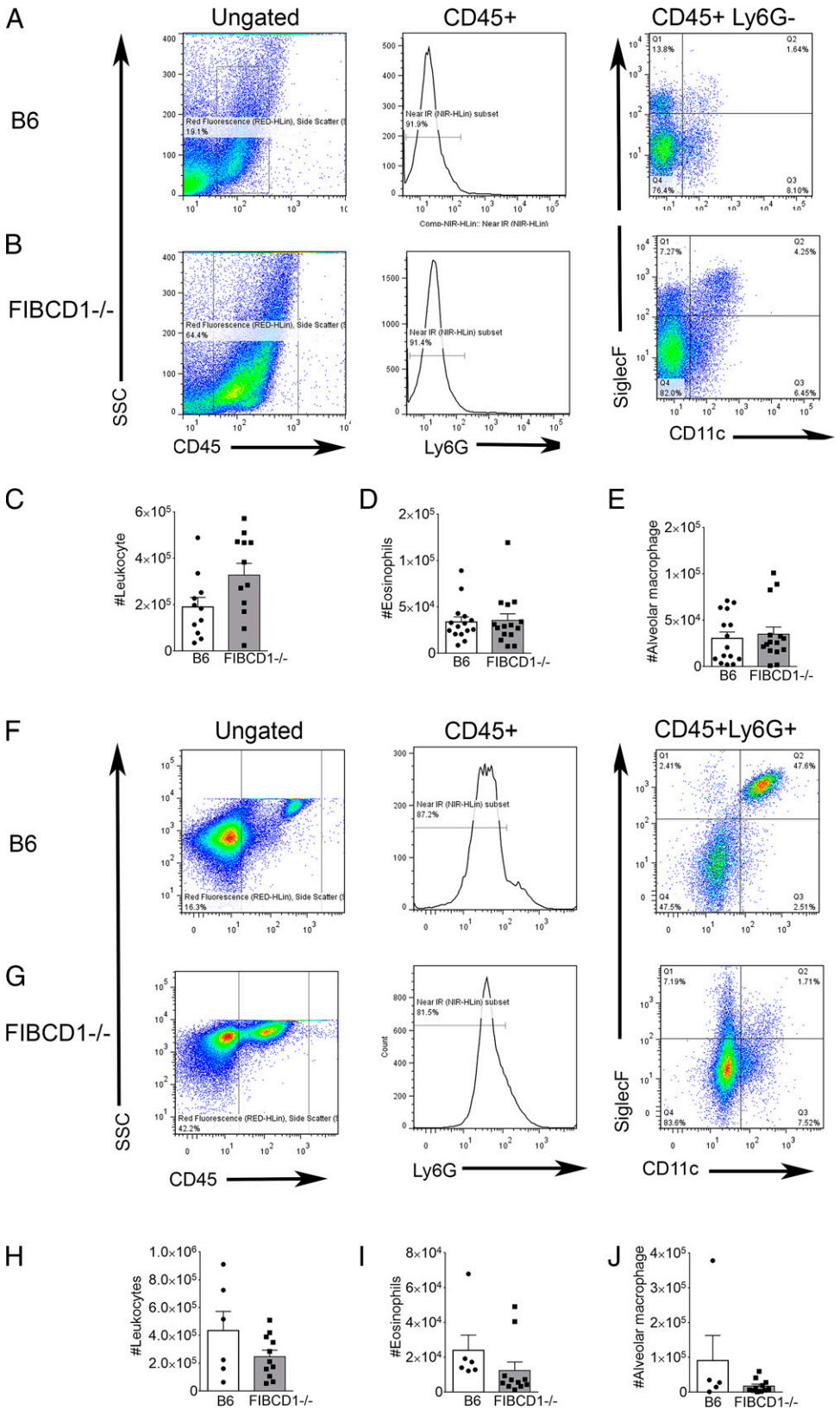


**FIGURE 4. No significant difference in recruitment of inflammatory cells in absence of FIBCD1 in IPA.**

(**A**–**J**) Fibcd1$^{-/-}$ and wild-type B6 mice were made immunocompromised by Ab depletion (clone 1A8) of neutrophils (A–E) or through pharmacological treatment (cyclophosphamide) (F–J) and then were infected with $1 \times 10^7$ Af293 fungal conidia as described in *Materials and Methods*. BALF was analyzed for polymorphonuclear cell recruitment. (A, B, F, and G) Representative flow plots depicting gating of BALF of control (A and F) and Fibcd1$^{-/-}$ (B and G) mice. (C–E and H–J) Graphical representation of the total population of CD45$^+$ leukocytes (C and H), CD45$^+$Ly6G$^-$Siglec-F$^+$CD11c$^-$ eosinophils (D and I), and CD45$^+$Ly6G$^-$Siglec-F$^+$CD11c$^+$ alveolar macrophages (E and J). Data shown are a summary of three or four experiments. *$p < 0.05$, **$p < 0.01$.

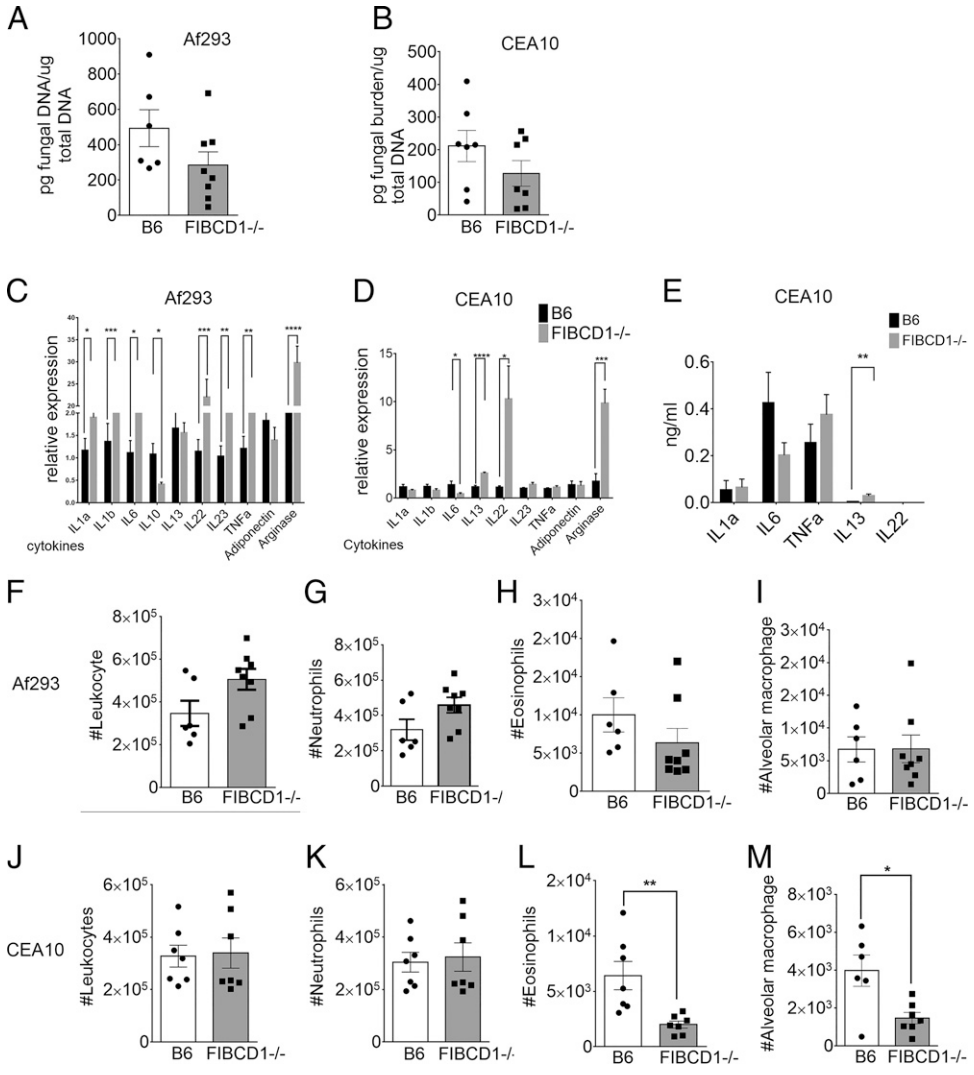


**FIGURE 5. Increased cytokine production in immunocompetent Fibcd1$^{-/-}$ mice in response to *A. fumigatus* aspiration.**

Mice of both groups aspirated 5 × $10^7$ conidia of either Af293 or CEA10 *Aspergillus* strains. (**A** and **B**) Fungal burden was quantified from lungs of both groups, harvested at 24 h postinfection: Af293 (A), CEA10 (B). (**C** and **D**) mRNA was extracted from harvested lungs and analyzed by qRT-PCR for expression of indicated cytokines: Af293 (C), CEA10 (D). (**E**) Cytokine secretion in BALF of CEA10-challenged mice was quantified at the protein level by ELISA. (**F**–**M**) BALF was analyzed for polymorphonuclear cell recruitment: Af293 (F–I), CEA10 (J–M). Graphical representations are shown of total populations of CD45$^+$ leukocytes (F and J), CD45$^+$Ly6G$^+$ neutrophil populations (G and K), CD45$^+$Ly6G$^-$Siglec-F$^+$CD11c$^-$ BALF eosinophils (H and L), and CD45$^+$Ly6G$^-$Siglec-F$^+$CD11c$^+$ alveolar macrophages (I and M). $n$ = 6–10 mice per group. Data are a summary of two to three independently performed experiments. *$p$ < 0.05, **$p$ < 0.01, ***$p$ < 0.001, ****$p$ < 0.0001.

## Cytokine modulation in immune-competent Fibcd1$^{-/-}$ mice after *A. fumigatus* aspiration

Our results in Figs. 1–4 suggest a detrimental role for FIBCD1 in IPA. However, it remains unknown whether this role is dependent on an immune-deficient phenotype. To determine the role of FIBCD1 in an immune-competent (or non–neutrophil-depleted) model of fungal inhalation, immune-competent mice were challenged with a single dose of 5 × $10^7$ *A. fumigatus* conidia. Af293 and the more virulent CEA10 strains were administered to wild-type and Fibcd1$^{-/-}$ mice by involuntary aspiration. Lungs were harvested 24 h postchallenge to quantify fungal burden and cytokine gene expression. Fungal burden in the Fibcd1$^{-/-}$ mice that aspirated a single dose of either Af293 or CEA10 conidia was not significantly decreased (Fig. 5A, 5B). Similar to infected neutropenic mice, IL-22 was increased in Fibcd1$^{-/-}$ mice compared with wild-type mice in response to Af293 and CEA10 (Fig. 5C, 5D). However, in contrast to neutropenic mice (Fig. 2), IL-1, IL-6, IL-23, and TNF transcripts were also increased in Fibcd1$^{-/-}$ mice when compared with wild-type mice, although less significantly in response to CEA10 (Fig. 5C, 5D). This trend was also suggested at the protein level in BALF supernatants of CEA10-challenged mice, but among the cytokines measured only IL-13 was significantly increased in Fibcd1$^{-/-}$ mice (Fig. 5E). Furthermore, BALF leukocytes, neutrophils, eosinophils, and alveolar macrophages were not different in response to Af293 (Fig. 5F–I), although eosinophils and alveolar macrophages were decreased in Fibcd1$^{-/-}$ mice challenged with the more virulent CEA10 strain, compared with wild-type controls (Fig. 5J–M). Wild-type and Fibcd1$^{-/-}$ mice challenged with CEA10 conidia did not exhibit differences in LDH cytotoxicity or albumin leakage in the lungs (data not shown). Our results show that immune-competent Fibcd1$^{-/-}$ mice respond to fungal aspiration with increased inflammatory cytokine gene expression compared with wild-type mice and neutropenic Fibcd1$^{-/-}$ mice, with only IL-22 increased with FIBCD1 deficiency in both models.

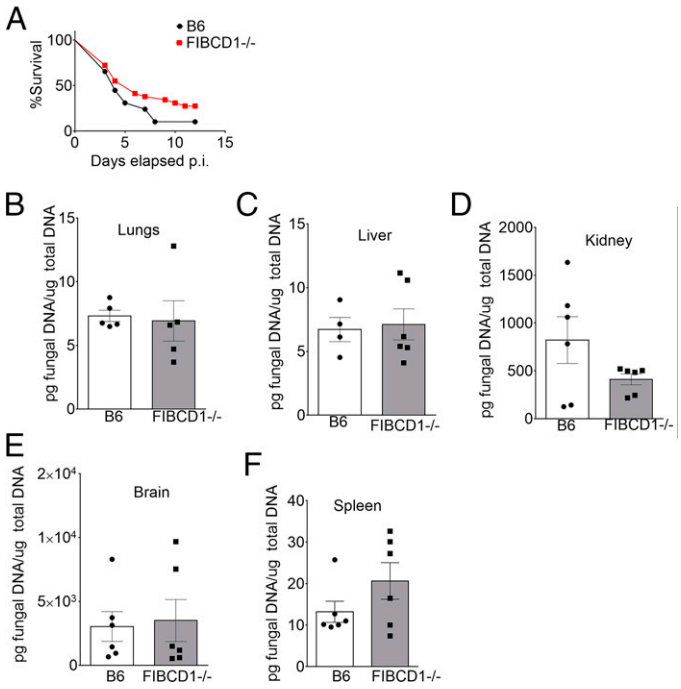


**FIGURE 6. Systemic i.v. infection in wild-type and Fibcd1$^{-/-}$ mice.** Mice of both groups were retro-orbitally infected with Af293 to induce systemic infection. (**A**) Survival score as described in *Materials and Methods*. (**B**–**F**) Quantification of fungal DNA from respective organ homogenates. Data are a summary of three to four independently performed experiments.

### *Comparison of wild-type and Fibcd1$^{-/-}$ mice in systemic fungal infection*

A serious complication of IA is fungal dissemination from the lungs to other organs, especially the brain, heart, and kidneys, and it is unknown whether Fibcd1 expression promotes systemic fungal infection. Therefore, we compared survival and fungal burden from multiple organs in immune-competent wild-type and Fibcd1$^{-/-}$ mice subjected to retro-orbital infection. During a 12-d postinfection, no statistically significant difference in mortality was observed in both groups (Fig. 6A). Similarly, no difference in fungal burden was observed in the lungs, liver, kidneys, brain, and spleen of wild-type and FIBCD1$^{-/-}$ mice (Fig. 6B–F). Thus, protection from IA gained by Fibcd1 deficiency cannot be extended from invasive lung infection to systemic infection.

### *Comparison of wild-type and Fibcd1$^{-/-}$ mice in a non-fungal lung injury model*

Next, we wanted to determine whether Fibcd1 deficiency could protect against lung injury in the absence of fungi. Therefore, we compared wild-type and Fibcd1$^{-/-}$ mice using the well-described bleomycin model of lung injury (24–26). At 30 d postinjury, we observed no difference in survival between wild-type and Fibcd1$^{-/-}$ mice with bleomycin-induced lung injury (Fig. 7A). Quantification of lung damage by an LDH cytotoxicity assay at days 6 and 13 postinjury also showed no differences (Fig. 7B–E), nor did we observe significant differences in airway leukocytes (Fig. 7F–M) and lung cytokines, with the exception of decreased TNF (Fig. 7O) in lavage fluid postinjury in Fibcd1$^{-/-}$ mice, and a significant drop in CD4$^{+}$ T cell–secreted IFN-γ was decreased in Fibcd1$^{-/-}$ mice at the initial stage of injury (Supplemental Fig. 3). We did observe a significant decrease in lymphocyte populations in lung homogenates (Supplemental Fig. 4) and noted a slight decrease of tissue-resident TNF-producing cells, both in lavage fluid and lung tissues, and a significant decrease in TNF in lungs of Fibcd1$^{-/-}$ mice compared with wild-type mice, on the later phase of injury (Supplemental Fig. 4), consistent with the decrease in TNF observed in knockout mice at the late phase of injury (Fig. 7E). These results demonstrate that FIBCD1 deficiency does not confer protection from bleomycin-induced lung injury.

## DISCUSSION

Previous studies have observed FIBCD1 protein expression to be localized on the apical site of human bronchial and alveolar epithelium, with chitin-binding capabilities associated with fungal colonization and inhibition of chemically induced gut inflammation (13, 14). Moreover, FIBCD1 has been shown to modulate cytokine secretion of airway epithelial cells in vitro (13–17). Therefore, it was important to investigate the role of FIBCD1 in lung immunity and infection with the chitin-containing *A. fumigatus*. In our study, we demonstrate a detrimental role of FIBCD1 in IPA, with decreased morbidity and mortality in Fibcd1$^{-/-}$ mice rendered immune compromised by Ab-mediated depletion of neutrophils or by treatment with cyclophosphamide. Fungal histological staining at days 1 and 3 postinfection demonstrated similar fungal burden at day 1 in wild-type and Fibcd1$^{-/-}$ mice, with decreased fungal growth likely due to increased clearance in Fibcd1$^{-/-}$ mice by day 3. Increased mortality and fungal burden by FIBCD1 appeared to be confined to lung infection in IPA, as we observed no significant differences in survival between groups in a systemic model of aspergillosis. Despite decreased pathology in IPA in the absence of FIBCD1, we observed no differences in airway inflammatory cells. Inflammatory cytokines were decreased in the absence of FIBCD1 in mice with IPA, consistent with decreased fungal burden.

Although no significant differences were observed in lung fungal burden in immune-competent mice in response to *A. fumigatus* aspiration, expression levels of candidate inflammatory cytokines were significantly increased in knockout mice, in contrast with the decreases observed in immunocompromised animals. This may reflect altered cytokine secretion due to neutrophil depletion or pharmacological inhibition in mice with IPA, whereas in immune-competent mice, cytokine secretion may be more effective in mediating fungal clearance and protection from infection and thus enhanced in Fibcd1$^{-/-}$ mice. Similarly, neutrophil depletion altered lung cytokine production in mice infected with *Cryptococcus neoformans*, although neutrophil depletion enhanced fungal clearance

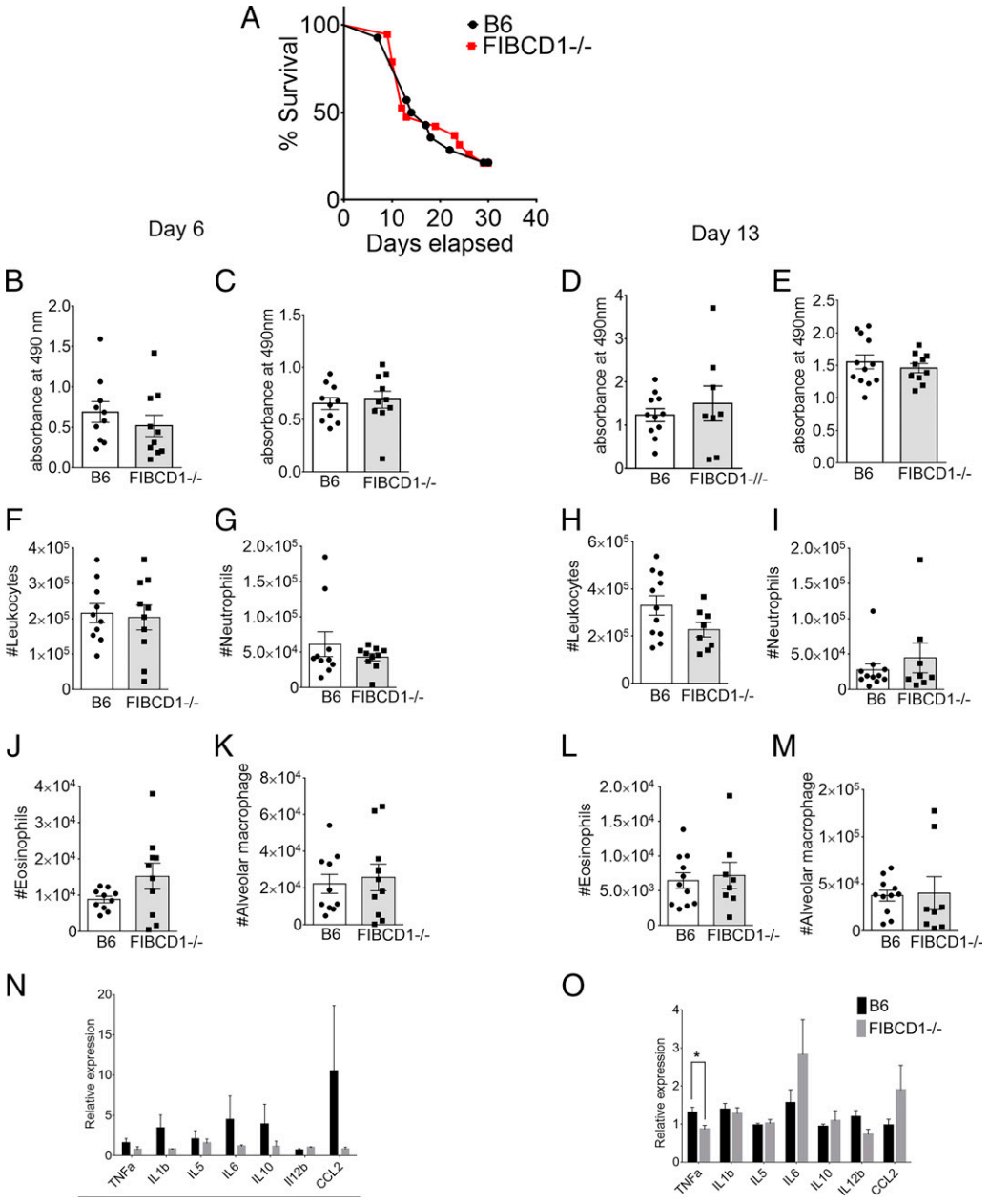


**FIGURE 7. Comparison of bleomycin-induced lung injury in wild-type and Fibcd1$^{-/-}$ mice.**

(**A**) Lung injury was induced in wild-type and knockout mice, and their survival was noted. (**B**–**E**) BALF and lungs were harvested at two different time points after injury (days 6 and 13) to assess fibrosis by LDH quantification of BALF (B and D) and lung tissue (C and E) at days 6 (B and C) and 13 (D and E). (**F**–**M**) Recruitment of polymorphonuclear cells in BALF at days 6 (F,G, J, and K) and 13 (H, I, L, and M) postinjury. Graphical representations are shown of total population of CD45$^+$ leukocytes (F and H), CD45$^+$Ly6G$^+$ neutrophil populations (G and K), CD45$^+$Ly6G$^-$Siglec-F$^+$CD11c$^-$ BALF eosinophils (J and L), and CD45$^+$ Ly6G$^-$Siglec-F$^+$CD11c$^+$ alveolar macrophages (K and M). (**N** and **O**) mRNA was harvested from injured lungs of bleomycin-treated mice of both groups, at days 6 (N) and 13 (O) post-challenge and analyzed by qRT-PCR for expression of the indicated cytokines. Data are a summary of two to three experiments. $n = 10$–12 mice per group. *$p < 0.05$.

(27), in contrast to the requirement for neutrophils in *A. fumigatus* clearance (1).

The mechanism by which FIBCD1 increases mortality, fungal burden, and inflammatory cytokine expression in mice with IPA is further complicated by difficulty in detecting tissue distribution of FIBCD1 protein expression in wild-type mice (data not shown), whereas in humans FIBCD1 is clearly expressed in epithelial tissues (13). In the gut, transgenic expression of epithelial FIBCD1 (mimicking conditions observed in humans) modulated fungal colonization and reduced disease severity in DSS-induced gut injury (14). This would appear in contrast to our study, where FIBCD1 deletion reduced disease severity in IPA. Hence, we wanted to determine whether a detrimental role for FIBCD1 in a lung infection model is broadly applicable in a bleomycin-induced model of lung injury, similar to DSS-induced injury in the gut. Pulmonary fibrosis is a chronic, irreversible, progressive, incurable interstitial lung condition with a poor prognosis and high mortality rate (25, 28, 29). It results from repetitive or ongoing injury to the alveolar epithelium, in which the repair process cannot complete normal re-epithelization, resulting in alveolar capillary damage. In contrast to FIBCD1-mediated protection from DSS-induced injury, we did not find any significant effect due to FIBCD1 on bleomycin-induced lung injury.

Our study describes a detrimental role for FIBCD1 in pulmonary fungal infection. However, the mechanism of FIBCD1-

mediated pathology remains unknown, and it remains a challenge to identify FIBCD1-mediated pathology beyond individual IA models, considering their heterogeneity and inherent limitations (30). Furthermore, the roles of FIBCD1 in chitin binding, fungal clearance, and modulation of cytokine secretion and signaling remain important directions for future studies. To answer these questions, the development of a model of humanized lung expression of FIBCD1 in mice, as was previously done in the gut (14), may be a promising strategy that will help determine whether FIBCD1 is a candidate target for therapies in immune-compromised patients with fungal infection.

## DISCLOSURES

The authors have no financial conflicts of interest.

## ACKNOWLEDGMENTS

We thank Amber Wilcox and Angar Tsoggerel for technical assistance, and Joe Lewis for animal care.

## REFERENCES

1. Hohl, T. M., and M. Feldmesser. 2007. *Aspergillus fumigatus*: principles of pathogenesis and host defense. *Eukaryot. Cell* 6: 1953–1963.
2. Kwon-Chung, K. J., and J. A. Sugui. 2013. *Aspergillus fumigatus*—what makes the species a ubiquitous human fungal pathogen? *PLoS Pathog.* 9: e1003743.
3. Latgé, J. P. 2007. The cell wall: a carbohydrate armour for the fungal cell. *Mol. Microbiol.* 66: 279–290.
4. Drummond, R. A., and G. D. Brown. 2011. The role of Dectin-1 in the host defence against fungal infections. *Curr. Opin. Microbiol.* 14: 392–399.
5. Lenardon, M. D., C. A. Munro, and N. A. R. Gow. 2010. Chitin synthesis and fungal pathogenesis. *Curr. Opin. Microbiol.* 13: 416–423.
6. Amarsaikhan, N., and S. P. Templeton. 2015. Co-recognition of β-glucan and chitin and programming of adaptive immunity to *Aspergillus fumigatus*. *Front. Microbiol.* 6: 344.
7. Aimanianda, V., J. Bayry, S. Bozza, O. Kniemeyer, K. Perruccio, S. R. Elluru, C. Clavaud, S. Paris, A. A. Brakhage, S. V. Kaveri, et al. 2009. Surface hydrophobin prevents immune recognition of airborne fungal spores. [Published erratum appears in 2010 *Nature* 465: 966.] *Nature* 460: 1117–1121.
8. Kousha, M., R. Tadi, and A. O. Soubani. 2011. Pulmonary aspergillosis: a clinical review. *Eur. Respir. Rev.* 20: 156–174.
9. Ostrosky-Zeichner, L., A. Casadevall, J. N. Galgiani, F. C. Odds, and J. H. Rex. 2010. An insight into the antifungal pipeline: selected new molecules and beyond. *Nat. Rev. Drug Discov.* 9: 719–727.
10. Dockrell, D. H. 2008. Salvage therapy for invasive aspergillosis. *J. Antimicrob. Chemother.* 61(Suppl 1): i41–i44.
11. Latgé, J. P., and A. Beauvais. 2014. Functional duality of the cell wall. *Curr. Opin. Microbiol.* 20: 111–117.
12. Clemons, K. V., J. E. Lutz, and D. A. Stevens. 2001. Efficacy of recombinant gamma interferon for treatment of systemic cryptococcosis in SCID mice. *Antimicrob. Agents Chemother.* 45: 686–689.
13. Jepsen, C. S., L. K. Dubey, K. B. Colmorten, J. B. Moeller, M. A. Hammond, O. Nielsen, A. Schlosser, S. P. Templeton, G. L. Sorensen, and U. Holmskov. 2018. FIBCD1 binds *Aspergillus fumigatus* and regulates lung epithelial response to cell wall components. *Front. Immunol.* 9: 1967.
14. Moeller, J. B., I. Leonardi, A. Schlosser, A. L. Flamar, N. J. Bessman, G. G. Putzel, T. Thomsen, M. Hammond, C. S. Jepsen, K. Skjødt, et al. 2019. Modulation of the fungal mycobiome is regulated by the chitin-binding receptor FIBCD1. *J. Exp. Med.* 216: 2689–2700.
15. Schlosser, A., T. Thomsen, J. B. Moeller, O. Nielsen, I. Tornøe, J. Mollenhauer, S. K. Moestrup, and U. Holmskov. 2009. Characterization of FIBCD1 as an acetyl group-binding receptor that binds chitin. *J. Immunol.* 183: 3800–3809.
16. Shrive, A. K., J. B. Moeller, I. Burns, J. M. Paterson, A. J. Shaw, A. Schlosser, G. L. Sorensen, T. J. Greenhough, and U. Holmskov. 2014. Crystal structure of the tetrameric fibrinogen-like recognition domain of fibrinogen C domain containing 1 (FIBCD1) protein. *J. Biol. Chem.* 289: 2880–2887.
17. Thomsen, T., J. B. Moeller, A. Schlosser, G. L. Sorensen, S. K. Moestrup, N. Palaniyar, R. Wallis, J. Mollenhauer, and U. Holmskov. 2010. The recognition unit of FIBCD1 organizes into a noncovalently linked tetrameric structure and uses a hydrophobic funnel (S1) for acetyl group recognition. *J. Biol. Chem.* 285: 1229–1238.
18. Amarsaikhan, N., E. M. O'Dea, A. Tsoggerel, H. Owegi, J. Gillenwater, and S. P. Templeton. 2014. Isolate-dependent growth, virulence, and cell wall composition in the human pathogen *Aspergillus fumigatus*. *PLoS One* 9: e100430.
19. O'Dea, E. M., N. Amarsaikhan, H. Li, J. Downey, E. Steele, S. J. Van Dyken, R. M. Locksley, and S. P. Templeton. 2014. Eosinophils are recruited in response to chitin exposure and enhance Th2-mediated immune pathology in *Aspergillus fumigatus* infection. *Infect. Immun.* 82: 3199–3205.
20. Swiatek, P. J., and T. Gridley. 1993. Perinatal lethality and defects in hindbrain development in mice homozygous for a targeted mutation of the zinc finger gene Krox20. *Genes Dev.* 7: 2071–2084.
21. Amarsaikhan, N., E. M. Sands, A. Shah, A. Abdolrasouli, A. Reed, J. E. Slaven, D. Armstrong-James, and S. P. Templeton. 2017. Caspofungin increases fungal chitin and eosinophil and γδ T cell-dependent pathology in invasive aspergillosis. *J. Immunol.* 199: 624–632.
22. Amarsaikhan, N., A. Tsoggerel, C. Hug, and S. P. Templeton. 2019. The metabolic cytokine adiponectin inhibits inflammatory lung pathology in invasive aspergillosis. *J. Immunol.* 203: 956–963.
23. Rao, G. V., S. Tinkle, D. N. Weissman, J. M. Antonini, M. L. Kashon, R. Salmen, L. A. Battelli, P. A. Willard, M. D. Hoover, and A. F. Hubbs. 2003. Efficacy of a technique for exposing the mouse lung to particles aspirated from the pharynx. *J. Toxicol. Environ. Health A* 66: 1441–1452.
24. Adamson, I. Y., C. Hedgecock, and D. H. Bowden. 1990. Epithelial cell-fibroblast interactions in lung injury and repair. *Am. J. Pathol.* 137: 385–392.
25. Izbicki, G., M. J. Segel, T. G. Christensen, M. W. Conner, and R. Breuer. 2002. Time course of bleomycin-induced lung fibrosis. *Int. J. Exp. Pathol.* 83: 111–119.
26. Jensen, K., K. P. Lund, K. B. Christensen, A. T. Holm, L. K. Dubey, J. B. Moeller, C. S. Jepsen, A. Schlosser, L. Galgóczy, S. Thiel, et al. 2017. M-ficolin is present in *Aspergillus fumigatus* infected lung and modulates epithelial cell immune responses elicited by fungal cell wall polysaccharides. *Virulence* 8: 1870–1879.
27. Mednick, A. J., M. Feldmesser, J. Rivera, and A. Casadevall. 2003. Neutropenia alters lung cytokine production in mice and reduces their susceptibility to pulmonary cryptococcosis. *Eur. J. Immunol.* 33: 1744–1753.
28. Kuhn, C. 1991. Patterns of lung repair. A morphologist's view. *Chest* 99(3, Suppl): 11S–14S.
29. Nici, L., A. Santos-Moore, C. Kuhn, and P. Calabresi. 1998. Modulation of bleomycin-induced pulmonary toxicity in the hamster by the antioxidant amifostine. *Cancer* 83: 2008–2014.
30. Desoubeaux, G., and C. Cray. 2018. Animal models of aspergillosis. *Comp. Med.* 68: 109–123.